Spicule formation in the gorgonian coral Pseudoplexaura flagellosa. 1: Demonstration of intracellular and extracel....

Article *in* Bulletin of Marine Science -Miami- · March 1987

CITATIONS
27

READS
73

2 authors:

Walter Goldberg
Florida International Un...
44 PUBLICATIONS **1,092** CITATIONS

SEE PROFILE

Yehuda Benayahu
Tel Aviv University
245 PUBLICATIONS **5,250** CITATIONS

SEE PROFILE

SPICULE FORMATION IN THE GORGONIAN CORAL *PSEUDOPLEXAURA FLAGELLOSA*. 1: DEMONSTRATION OF INTRACELLULAR AND EXTRACELLULAR GROWTH AND THE EFFECT OF RUTHENIUM RED DURING DECALCIFICATION

Walter M. Goldberg and Yehuda Benayahu

ABSTRACT

Spicule formation in the gorgonian *Pseudoplexaura flagellosa* (Houttuyn) is a complex event involving a transient intracellular step followed by a longer process of extracellular growth. The intracellular phase produces electron lucent vesicles 1–2 μm in diameter that are closely associated with mitochondria and the Golgi apparatus. The vesicles calcify and enlarge, forming one or more intracellular masses of polymorphic crystals that are released to the extracellular space or mesoglea. These calcified structures, the spicule primordia, serve as the focal points for continued growth through the agency of secondary sclerocytes in the mesoglea. Secondary sclerocytes do not form crystals within vesicles. Instead, several of these cells form a complex network of interdigitating, overlapping pseudopodia surrounding the primordia. Crystal formation appears to occur within the space between membrane and spicule although details of the process are not clear. The result of secondary growth is the integration of several primordia into a single immature spicule by formation of overlapping, concentric sheets of blade-like calcite crystals. As secondary growth continues, additional secondary sclerocytes settle on the spicular surface creating complex tubercles. The last step of spicule formation is characterized by a perispicular envelope created by the pseudopodia of separate but closely apposed secondary sclerocyte daughter cells. This stage produces the final layers of secondary growth over the entire spicule surface, sealing in the tubercular structures. Mature spicules are free of cellular material.

Additional experiments demonstrate that ruthenium red has a stabilizing influence on the spicule matrix, preventing its complete extraction during decalcification. Ruthenium red exerts its primary influence extracellularly and does not ordinarily prevent loss of matrix from the intracellular phase of primordium formation. These data support the morphological evidence that spicule formation in *P. flagellosa* is initially intracellular but is primarily an extracellular, multicellular event.

Virtually all octocorals form calcified materials. In some specialized groups the axial skeleton is calcified, either with amorphous carbonate or with fused or aggregated spicular elements (Bayer, 1955; Franc et al., 1974; Ledger and Franc, 1978; Kingsley and Watabe, 1982a; Grasshoff and Zibrowius, 1983). More commonly spicules are found as unfused, individual structures that occur in tracts within octocoral cell clusters or mesoglea.

Electron microscopic studies of spicule formation have suggested the occurrence of different cellular patterns in different species. Kawaguti (1964) and Kawaguti and Kamishima (1973) suggested that spicules were initiated by calcifying intracellular vesicles that become extracellular. Spicules form from several calcifying cells (sclerocytes) that presumably release their contents onto the surface of a growing spicule. Alternatively, Kawaguti (1969), Dunkelberger and Watabe (1974), and Kingsley and Watabe (1982b) have argued that spicules in various octocorals grow and mature primarily, and possibly entirely within individual sclerocytes. The latter authors have also shown that spicules ultimately become extracellular structures.

The present contribution involves the study of spicule formation in the common reef dwelling gorgonian *Pseudoplexaura flagellosa* (Houttuyn, 1772). Our work

focuses on morphogenetic events involved in spicule formation, using a variety of microscopic techniques applied to calcified as well as decalcified material.

Materials and Methods

Uninjured branch tips of *Pseudoplexaura flagellosa,* and branches allowed to regenerate for 3 or 6 days in the field were collected from Key Largo, Florida. Fixation began within 15 min or less and continued for 4–6 h in a modified Karnovsky-type mixture (K) containing 4% paraformaldehyde, and 2% glutaraldehyde in 0.05 M cacodylate buffer, pH 7.6 or 8.0. Variations of this mixture employed additives to improve fixation including 0.1% tannic acid (TAK) (Simionescu and Simionescu, 1976), 0.05% picric acid (PAK) (Ito and Karnovsky, 1968) or 0.2% ruthenium red (RRK) (Shepard and Mitchell, 1977). The fixatives were brought to a tonicity equal to seawater (measured by specific gravity) with addition of concentrated artificial seawater. Subsequent processing included 1% osmium tetroxide (OsO_4) in cacodylate buffer for 1 h followed by graded ethanolic dehydration and infiltration with Spurr resin. RRK-fixed material was processed with 0.1% RR in the osmium according to the method of Shepard and Mitchell (1977). All steps were carried out at room temperature. Infiltration was improved by using low speed centrifugation ($< 100 \times g$) during two 20-min resin changes followed by final embedment employing a vacuum oven. Gold and silver thin sections were taken including those from specimens sectioned serially. These undecalcified sections were examined either unstained or after staining with lead citrate. Sections up to 1 μm thick were stained with toluidine blue and basic fuchsin according to the method of Alsop (1974).

Decalcification was often required due to severe dislocation of carbonate during sectioning, especially in mature spicules. The simplest successful technique employed 4% uranyl acetate in 50% ethanol en bloc for 24–48 h. Other methods of en bloc decalcification employed material fixed in the presence of ruthenium red and included use of 1% formic acid-sodium formate pH 3.5, 1% phosphotungstic acid, 5% ethylenediaminetetraacetic acid (EDTA) buffered to pH 7.6 with 0.05 M cacodylate (Bonucci and Reurink, 1978), triethylammonium EDTA (EA-EDTA), pH 7.6 (Scott and Kyffin, 1978) or 2% ascorbic acid-NaCl (Dietrich and Fontaine, 1975; Wakita et al., 1983). Gold and silver sections of decalcified material were stained with ethanolic uranyl acetate followed by lead citrate. Material examined included coenenchymal (non-polyp) tissue from both subepithelial and circumskeletal mesoglea, using a Philips 200 electron microscope operated at 60 kV. Light microscope observations were made on RRK-fixed material decalcified by EA-EDTA and stained according to Alsop (1974).

Spicules were prepared for scanning electron microscopy by placing short lengths of Karnovsky-fixed *P. flagellosa* branches in warm 1 N NaOH for 1 h to dissolve tissue, followed by decantation and repeated washings in water, and a final wash in methanol. Spicules were then treated by immersion in liquid nitrogen and brief, low pressure grinding in an agate mortar and pestle. After removal of fines by decantation of methanol, spicule fragments were mounted on double-stick tape, coated with Au/Pd and examined using an ISI 3A SEM. Energy dispersive X-ray analysis of whole spicules was performed on an ISI-DS 130 SEM (probe size—0.45 μm, accelerating voltage 35 kV) interfaced with a Tracor Northern 2000 elemental analyzer. X-ray diffraction analysis employed powdered spicules in a Philips XRG-3000 X-ray diffractometer operated in slow scan mode at 30 kV and 25 mA. Scans were performed between 29–30 degrees 2ϕ for calcite and 25–27 degrees for aragonite.

Results

The mesoglea of *P. flagellosa* contains a network of cell "cords" (Chester, 1913) composed of a variety of cell types. Dense aggregations of granular cells, mucus cells, nematocyst-forming cells (nematocytes), spicule-forming cells (sclerocytes) and zooxanthellae are the primary network components (Figs. 1 and 2).

Sclerocytes in early stages of crystal formation are found clustered near the edge of the cell cord. They typically possess tightly apposed, convoluted plasma membranes (Fig. 4), numerous mitochondria, Golgi bodies and a large number of cytoplasmic vesicles (Figs. 3 and 4). Some of these vesicles are derived from the Golgi complex and are closely associated with larger, mostly electron lucent vesicles. The latter structures are the sites of primary crystal formation (secondary crystal formation is extracellular as described below) and are referred to as calcifying vesicles (CV). The internal portions of the CV may contain fibrous material or traces of organic matter but this is not consistent among different preparations or even within single sections.

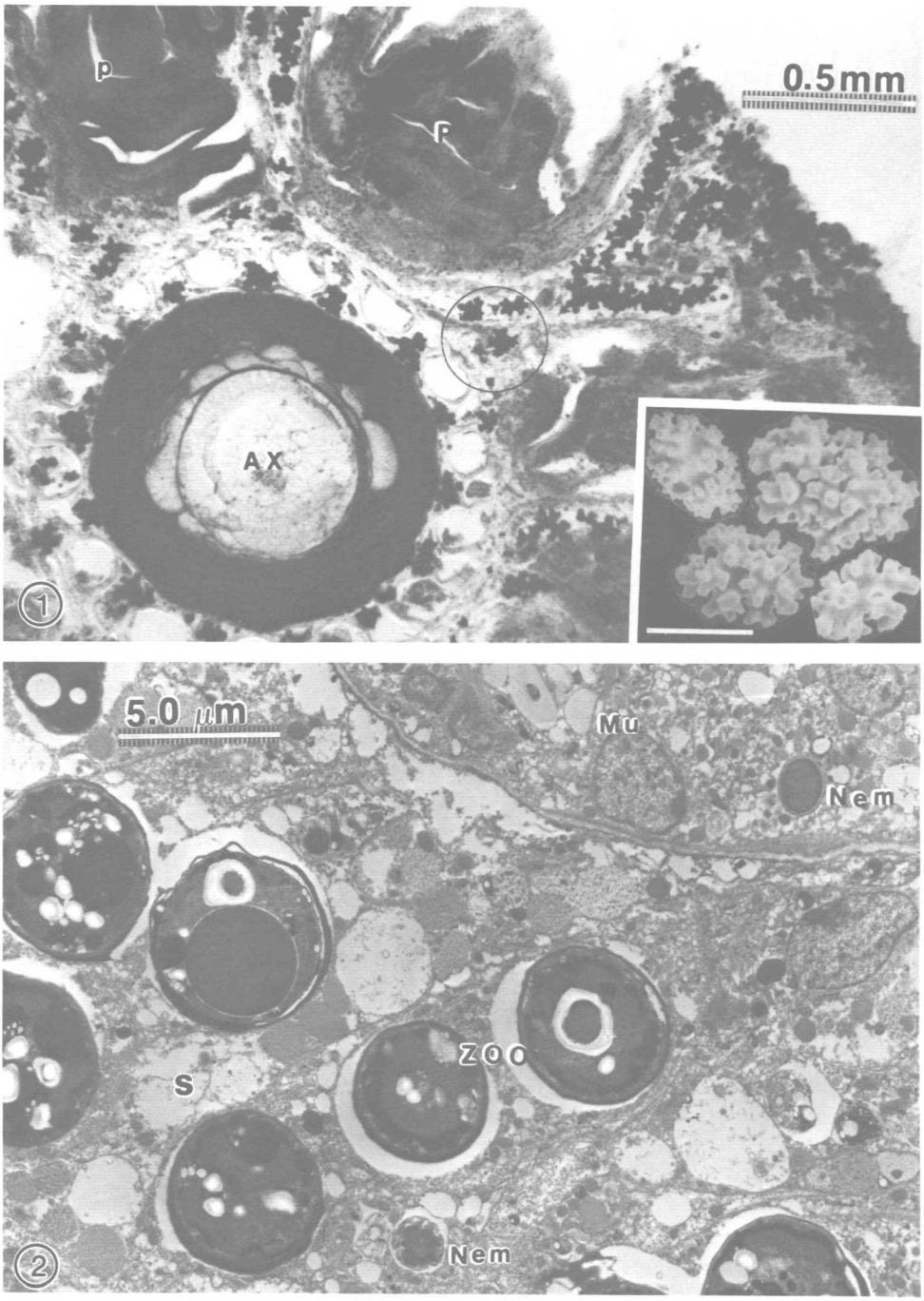

Figure 1. Cross section of *Pseudoplexaura flagellosa* branch showing relationship of axial skeleton (AX), polyps (P) and surrounding tracts of spicules. A mesogleal cell cord is circled. Cryostatic section, unfixed, unstained. Inset: SEM of spicules, bar = 100 μm.

Figure 2. Low power electron micrograph of cell cord region showing typical aggregation of zooxanthellae (ZOO), nematocytes (Nem), mucus cells (MU) and decalcified spicules (S). Decalcification by EDTA removed the spicule matrix in this preparation. PAK-OsO_4 fixation; no section stain.

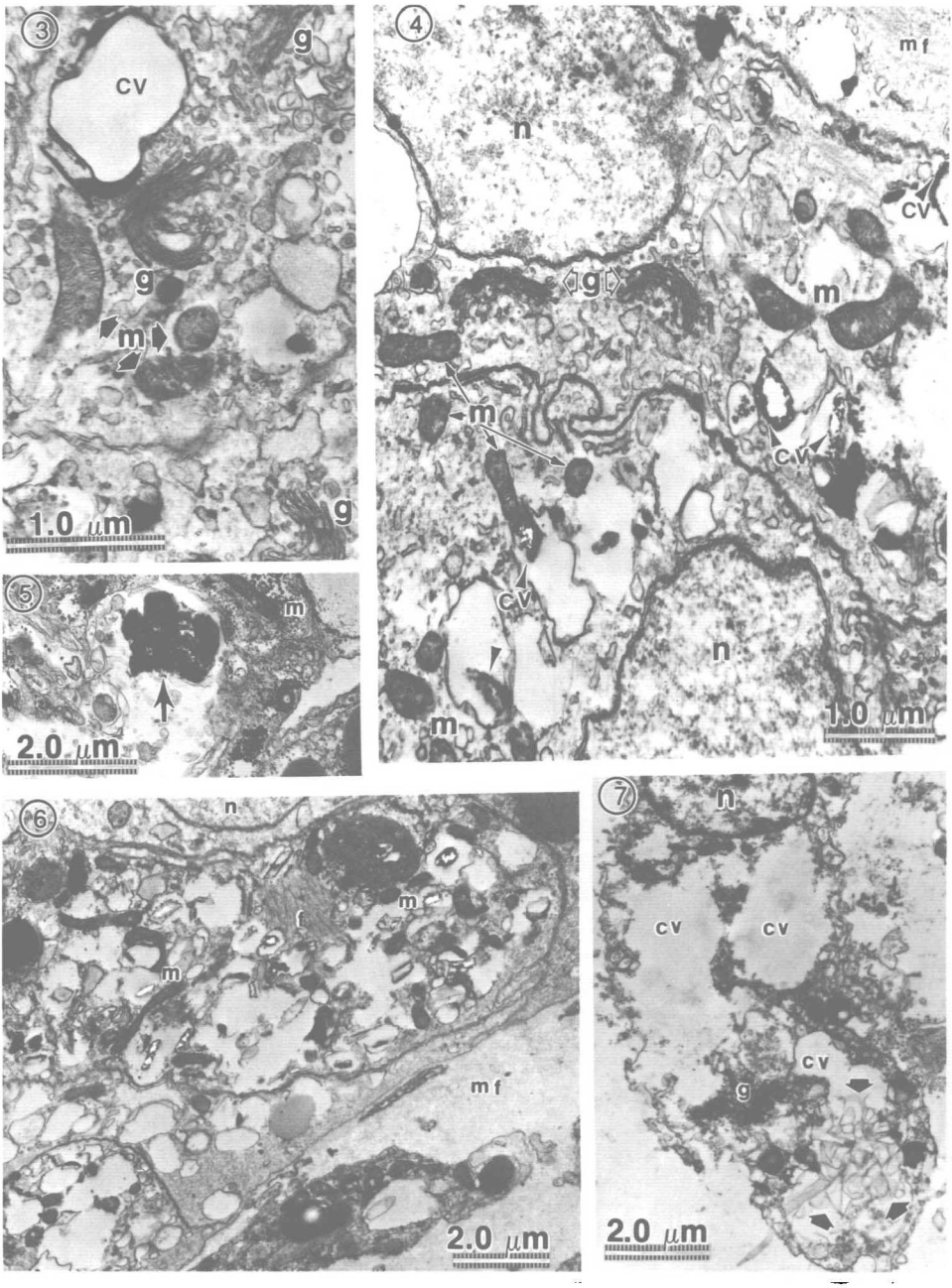

Figure 3. Sclerocyte with calcifying vesicle (CV) appearance before onset of mineralization. Large numbers of Golgi vesicles (g) and mitochondria (m) are associated with the CV. RRK, RRO fixation, undecalcified, Pb stain.

Figure 4. Part of an aggregation of scleroblasts. Calcified material appears in CV marked by arrows. Symbols as above. n = nucleus, mf = mesogleal fibers. Specimen preparation as above.

Figure 5. Mineralized material (arrow) with irregular outlines after release from sclerocyte. Specimen preparation as above.

Figure 6. Sclerocytes contain numerous calcifying vesicles that may fuse to form larger intracellular

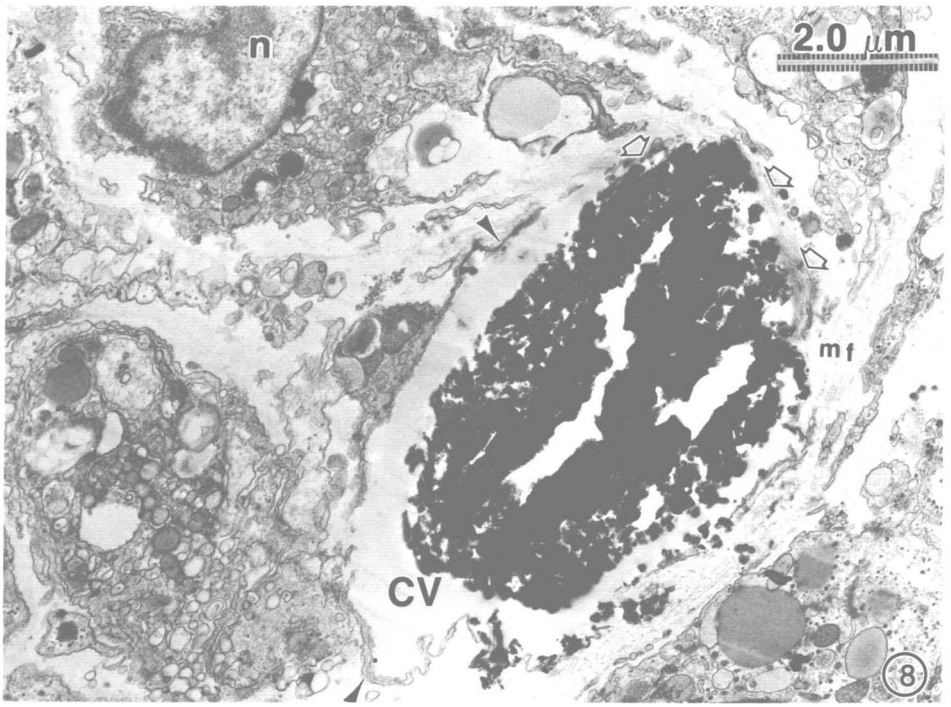

Figure 8. Sclerocyte with large deposit of carbonate becoming extracellular. Cell-membrane (dark arrows) has been breached allowing contact between carbonate and mesoglea (clear arrows). Note pseudopodial processes of neighboring secondary sclerocytes. RRK, RRO fixation, undecalcified, Pb stain.

The crystals and crystal outlines found within the CV display a variety of form and size ranging from blades 0.1 μm thick to rhomboid structures 0.5 μm or more in diameter (Figs. 4–7, 18 and 19). These irregular crystals proliferate within the 1–2 μm vesicles that may either fuse to form larger CV structures, or may be discharged to the extracellular space (Fig. 5). Sclerocytes that release smaller calcified structures do so by a process of exocytosis, leaving the cell intact. Conversely, and more typically, fusion produces 1–3 large, ovoid vesicles (Figs. 7 and 8). These structures also become extracellular but by a process accompanied by degeneration of the plasma membrane after fusion with vesicular membranes.

Cells that form crystals within vesicles are quite uncommon under ordinary conditions of growth, but proliferate in the first few days after injury. Specimens allowed to regenerate in the field for as long as 6 days prior to collection possess few of these "primary sclerocytes." They are also quite uncommon in undamaged branch tips, which characteristically have a substantial complement of mature or nearly mature spicules. The function of these apparently transient cells is to

←
vesicles. Fibrous material (f) typically occurs in these cells but usually not intravesicularly. Other symbols and specimen preparation as above.

Figure 7. Sclerocyte with Golgi (g)-associated CV's. Decalcification with ascorbic acid has extracted the organic matter in two vesicles despite use of ruthenium red. Outlines of irregular crystals (arrows) typically produced intracellularly are preserved in one vesicle.

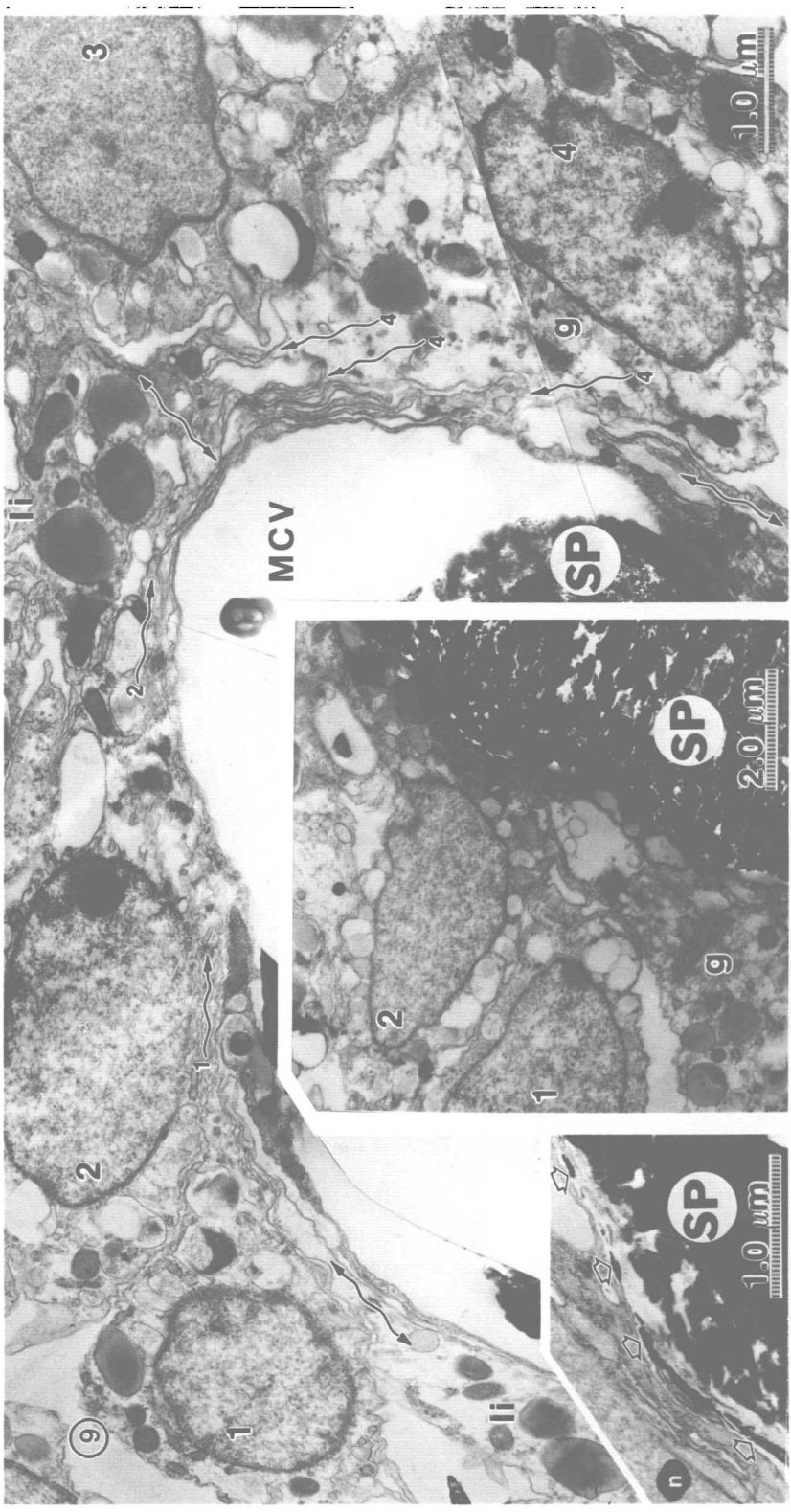

Figure 9. Multicellular (multi-pseudopodial) vesicle (MCV) containing calcified primordium reconstructed from serial sections. Numbered nuclei depict sclerocytes contributing pseudopodia with corresponding number. Double headed arrows mark pseudopodia from cells with nuclei outside the micrograph. Center inset: same MCV and cells cut perpendicularly. Overlapped pseudopodia on spicule surface are possible sites of calcification. Left inset: carbonate deposits between pseudopodia. n = nucleus, SP = spicule primordium, g = Golgi, li = lipoid inclusion, MCV = multicellular vesicle. Fixation and stain as in Figure 8.

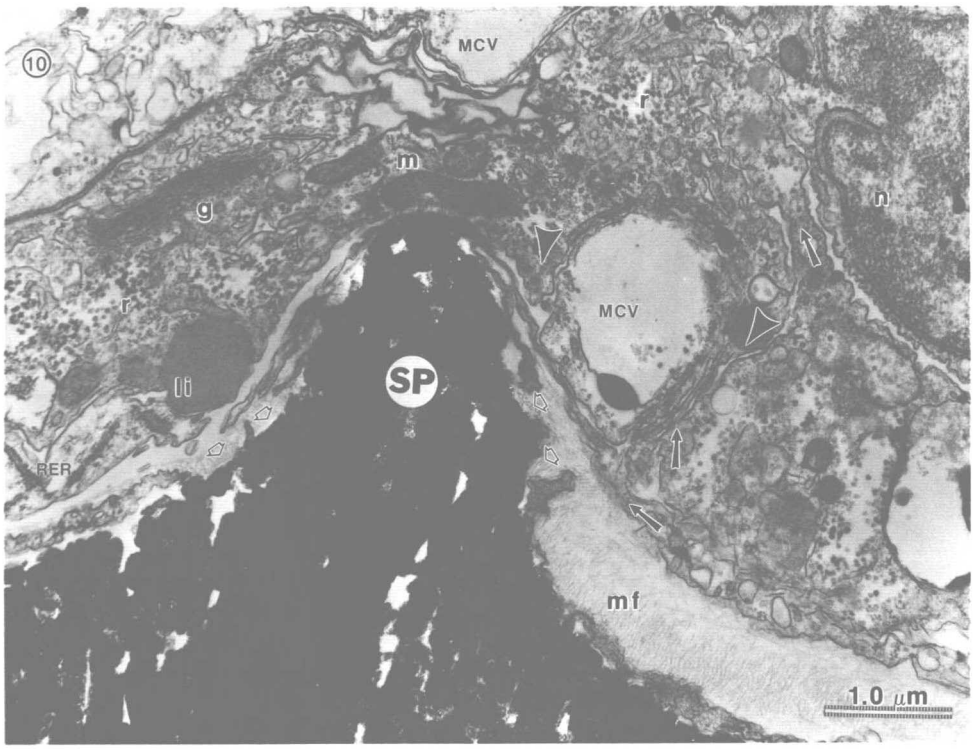

Figure 10. Multiple MCV structures with associated secondary sclerocytes. Cytoplasm contains numerous ribosomes (r) and lipoid material (li). Arrowheads pointing down show pseudopods contributing to an MCV from this cell; arrows from lower right show three additional pseudopods from an adjoining cell. Additional pseudopodia surround the carbonate. Clear arrows point to areas of contact by mesogleal fibers (mf). Formation of spicular tubercles may be represented here. Fixation and stain as Figure 9.

discharge one or more calcified primordia into the extracellular space, usually near the junction of a cell cord and mesoglea.

The extracellular primordia are contacted by cells within the mesoglea that, unlike primary sclerocytes, characteristically produce pseudopods (Fig. 8). These "secondary sclerocytes" are also distinguished by the presence of more numerous lipoid inclusions and larger numbers of free ribosomes. In early stages of growth only one or two such cells contact the extracellular carbonate, but subsequently, contact is made with multiple secondary sclerocytes. The plasma membranes of these cells form extremely thin pseudopodia that intersect and overlap in several planes. A multicellular (multi-pseudopodial) "vesicle" (MCV) forms from this arrangement and confines the mineralized material extracellularly. Figure 9 shows one such MCV and traces the cellular origin of the overlapped pseudopodia by reconstructing serial sections. The central inset of this figure shows the same MCV and cells cut perpendicularly. Overlapped pseudopodia on the surface of the spicular primordium form blister-like compartments, but no crystals can be distinguished within them (see also Fig. 18). If calcification occurred only on the surface of the extracellular carbonate, it would be difficult to distinguish new growth. Occasionally, however, mineral is deposited that is not in contact with the spicule but is clearly associated with a pseudopodium (Fig. 9 left inset). Although our data do not allow for a more precise description of carbonate depo-

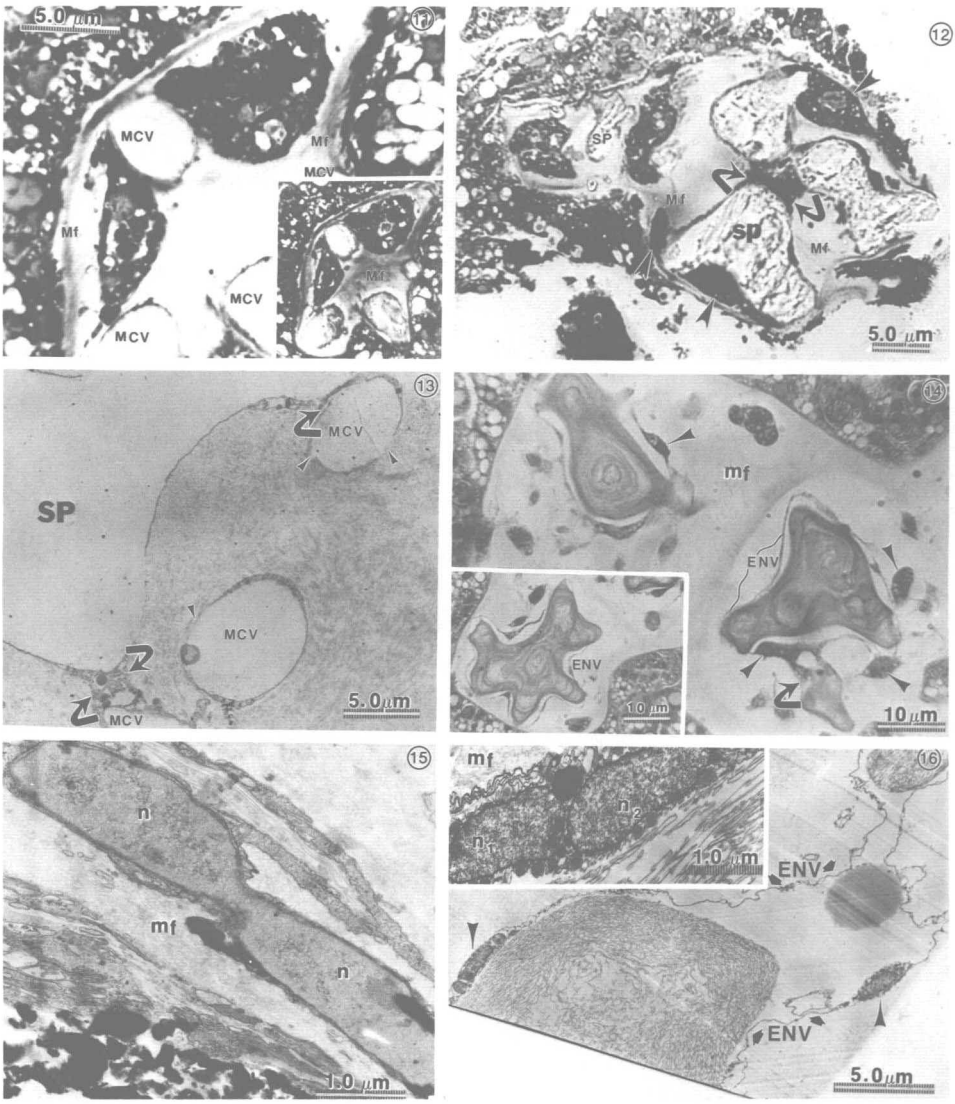

Figure 11. Light micrograph of multiple MCV with attendant overlapping sclerocytes, and surrounding mesogleal fibers (mf). RRF fixation, undecalcified, toluidine blue-basic fuchsin stain. Inset: overview of same.

Figure 12. Three MCV structures with appreciable secondary growth are joined by two sclerocytes (curved arrows) forming an immature spicule. Arrowheads point to cells surrounding spicule exterior. Mesogleal fibers (mf) surround the complex. Preparation as above.

Figure 13. Tubercles (warts) are formed by additional smaller MCV structures joining the surface of the main body of the spicule (SP). Curved arrows show cytoplasmic connections formed between calcified regions. Arrowheads point to contacts between carbonate and mesoglea. Note complete extraction of spicule matrix. K, Os fixation, EDTA decalcification, UA/Pb stain.

Figure 14. Light micrograph of decalcified maturing spicules. Arrowheads depict sclerocytes with nuclei; curved arrow shows cytoplasmic contact between two mineralized areas, possibly representing formation of a tubercle. These spicules are surrounded by an envelope (ENV) formed by secondary sclerocyte pseudopodia. RRK fixation, EA-EDTA decalcification, toluidine blue-basic fuchsin stain. Inset: spicule with tubercles surrounded by envelope.

sition, the arrangement of secondary crystals into overlapping sheets (see below) corresponds with the typical multilaminar structure of pseudopodia. Secondary sclerocytes do not form intracellular calcifying vesicles.

In later stages several MCV structures become associated by cell overlap. The sclerocyte with cytoplasm showing in Figure 10 is sandwiched with other cells (or folds of the same cell) between two masses of carbonate. Only one calcified area is shown. This sclerocyte also contributes pseudopodia to a third, smaller MCV seen on the right. These relationships can also be appreciated on the light microscope level where sections show large numbers of cell clusters in the mesoglea. The clusters are composed of secondary sclerocytes that interconnect several calcified primordia (Fig. 11). Mesogleal fibers, in turn, connect, surround and often define individual clusters. A subsequent stage is shown in Figure 12 in which three MCV structures are in close contact, separated only by small amounts of cytoplasm. This stage depicts the formation of an immature spicule, derived from integration of separate MCV's fused by secondary growth. As the main body of the spicule is formed in this way, additional, smaller MCV structures settle onto the spicular surface, thus greatly increasing its complexity by formation of tubercles or warts (Figs. 10, 13 and 14).

The final stages of spicule formation occur when parts of the spicule are no longer separated by cellular material. Secondary sclerocytes take on a fusiform appearance due to highly elongated pseudopodia, often so thin that the cytoplasm lacks sufficient space for vesicles and organelles. A prominent nucleus surrounded by numerous membrane bound, electron opaque vesicles constitutes most of the cell volume at this stage (Figs. 16 and 17). The relationship of these vesicles, if any, to the calcification process is not clear. The pseudopods of several fusiform cells enclose the entire spicule, forming a perispicular envelope. This structure is produced by secondary sclerocyte daughter cells (Figs. 15 and 16), separated by simple junctions ~15 nm apart (Fig. 17 inset). The appearance of the envelope is correlated with the final layering of secondary growth that seals the tubercles on the spicule surface (Fig. 17 inset). Mature spicules are up to 175 μm long; they are free of membranous structures and are in full contact with mesoglea.

Figure 18 shows the typical appearance of a decalcified spicule in cross section. The central portion, approximately 3–5 μm in diameter, contains a variety of crystal shapes judging from the remaining matrix. This part of the spicule corresponds with the general characteristics of a spicular primordium and represents the product of intracellular calcification. The primordium is surrounded by a more or less concentric arrangement suggesting that a more regular process of crystal deposition occurs extracellularly. The corresponding arrangement of crystals is shown by scanning electron microscopy of frozen-fractured spicules. Figure 19 is a cross section showing a primordium composed of an irregular crystalline mass approximately 5 μm in diameter. This in turn is surrounded by concentric layers of more regular crystals. Figure 20 shows more clearly that the concentrically arranged crystals are thin and flat, measuring 0.4 $\pm$ 0.2 μm wide and 0.1 $\pm$ 0.03 μm thick.

←

Figure 15. Secondary sclerocyte cell initiating nuclear division. RRK, RRO fixation, undecalcified, Pb stain.

Figure 16. Low power electron micrograph of perispicular envelope (ENV). Arrowheads point to nuclei and surrounding cytoplasmic vesicles. ×6,000. Inset: secondary sclerocyte with completed nuclei and surrounding cytoplasmic vesicles. Inset: secondary sclerocyte with completed nuclear division prior to cytokinesis. RRK, RRO fixation, en bloc UA decalcification. No section stain.

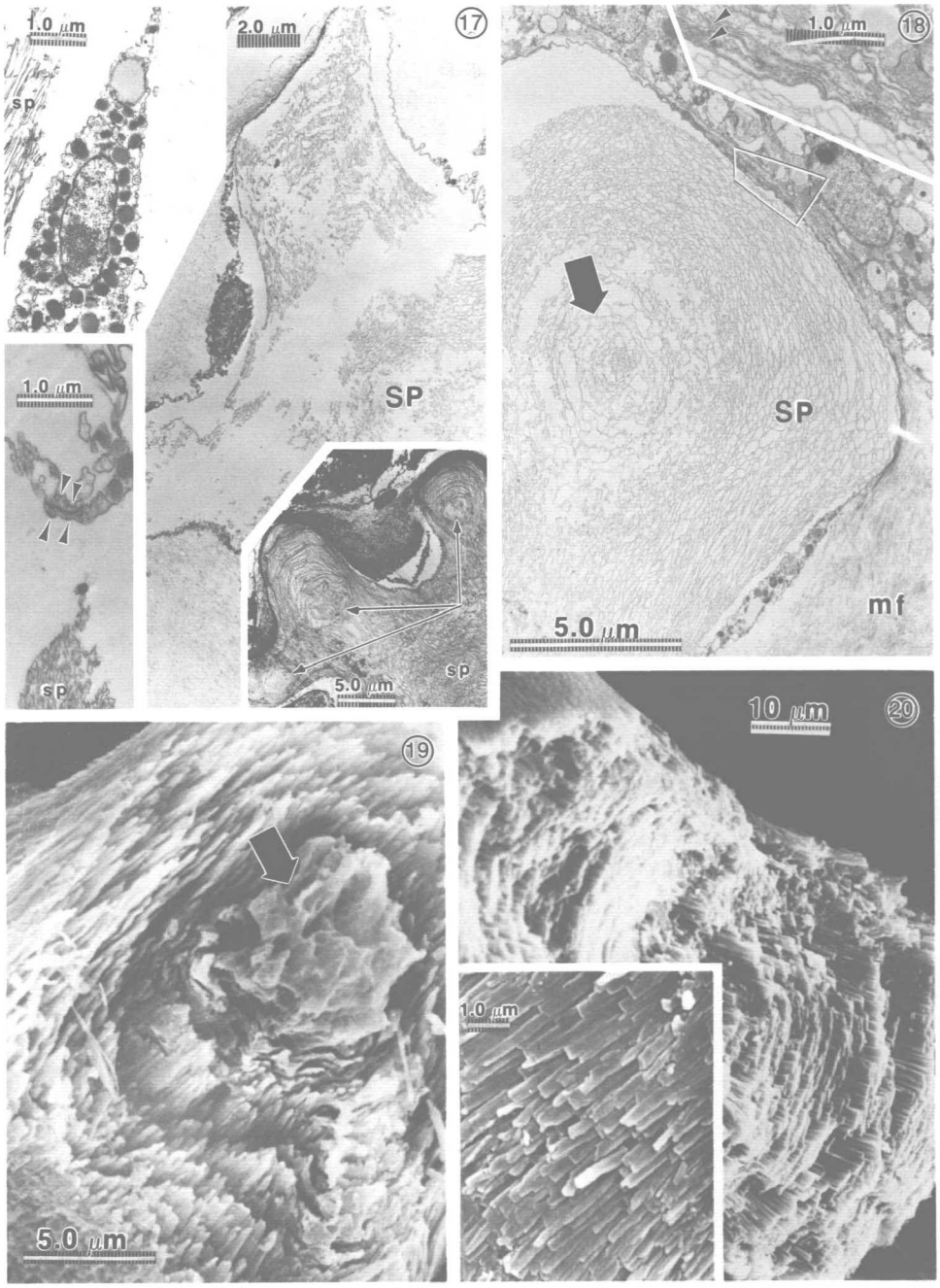

Figure 17. Center: perispicular envelope (TAK, OsO_4 fixation, en bloc UA decalcification, Pb stain). Upper left: details of perinuclear cytoplasm (RRK, RRO fixation, ascorbic acid decalcification, UA/Pb stain). Lower left: closely apposed simple cell junctions characteristic of the envelope (preparation as above). Lower right: secondary growth sealing in tubercular primordia indicated by arrows (K, OsO_4 fixation, en bloc UA decalcification, Pb stain). SP = decalcified spicule organic matrix.

Figure 18. Decalcified spicule cross section showing arrangement of irregularly shaped crystal outlines typical of intracellular (primordium) phase of spicule formation (arrow). The primordium is surrounded

Whole spicules ground to a powder give an X-ray diffraction pattern typical of calcite; no aragonite is detectable. Preliminary work using X-ray microanalysis suggests that only traces of magnesium and sulfur are present in addition to calcium.

Results of Decalcification Experiments.—Our initial attempts to decalcify spicules with aqueous or ethanolic EDTA, phosphotungstic acid, formic acid and ascorbic acid all resulted in complete extraction of the organic matrix, leaving behind what appeared to be holes in the mesoglea bound by pseudopodial membranes (Fig. 13). The pericrystalline outlines constituting the preserved portion of the spicular matrix (Figs. 14, 16–18) became solubilized and lost. Only uranyl acetate decalcification preserved the matrix. While we have not specifically examined the effect of uranyl acetate, we have found that virtually any form of decalcification can retain the matrix structure of the spicule as long as ruthenium red is employed in the primary fixative. The exception to this rule is among primary sclerocytes where decalcification ordinarily results in loss of matrix whether ruthenium red is employed or not. Figure 7 shows a primary sclerocyte from tissue fixed in the presence of ruthenium red, followed by decalcification with ascorbic acid. Two of three calcifying vesicles are devoid of matrix, while a third retains some of the irregular crystal outlines typical of primary sclerocytes. Such intracellular preservation is unusual.

In terms of ultrastructural quality, the best results are obtained when ruthenium red is employed in the fixative and either uranyl acetate or triethylammonium EDTA are used en bloc for decalcification. Acceptable results are obtained with ascorbic acid but the other reagents produce a wide range of artifacts (unpubl. data).

Discussion

Calcification microenvironments may be divided into four basic groups: (1) extracellular calcification between cells and a crystalline substratum, (2) extracellular calcification bound by epithelial tissues, (3) intracellular calcification within vesicles or vacuoles (Wilbur and Simkiss, 1979; Wilbur, 1980) and (4) intracellular calcification within a syncytium (Märkel and Röser, 1983; Stricker, 1985). It is also recognized that an organism may use more than one of the four groups in mineral deposition. As summarized in Figure 21, our study falls in this category, and is therefore similar to the formation of echinoderm spines and plates of the test (Shimizu and Yamada, 1980). In the latter case, crystal growth is initiated intracellularly within vesicles of primary sclerocytes and released to the extracellular space where subsequent growth is completed by secondary sclerocytes. The first phase appears to be a conventional case of intracellular calcification

←

by a more regular, somewhat concentric arrangement of crystal outlines. Magnified area (inset) shows detail of pseudopodia (arrowheads) tangent to the spicule surface. RRK, RRO fixation, EA-EDTA decalcification, UA/Pb stain.

Figure 19. Scanning electron micrograph of spicule fractured in liquid nitrogen. Interior of spicule shows an irregular core of mineralized material representing a spicule primordium produced intracellularly (arrow). More regular calcite crystals surrounding this structure are produced extracellularly.

Figure 20. Blade-like crystals of calcite are arranged concentrically around the primordium within the fractured spicule. Inset: outer surface of spicule shows overlapped sheets of crystals. Specimen preparation as above.

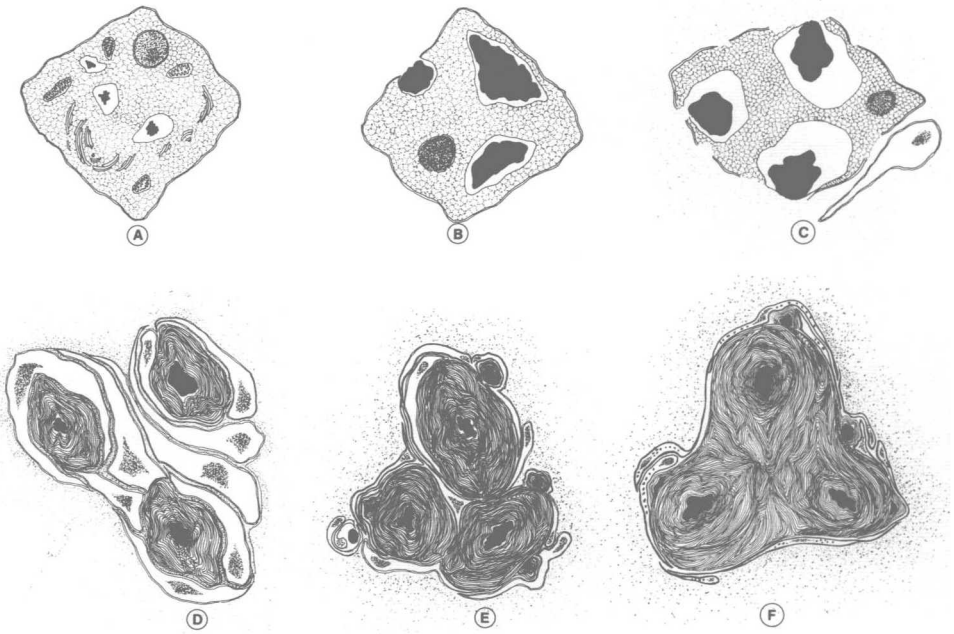

Figure 21. Hypothetical sequence of spicule formation by *Pseudoplexaura flagellosa*: A–C, Intracellular calcification and primordium formation. D, Secondary growth and MCV formation. E, Formation of tubercles and integration of MCV structures. F, Maturing spicule with cellular envelope.

within vesicles as reported for a wide variety of organisms including coelenterates (Kawaguti, 1964; Dunkelberger and Watabe, 1974; Spangenberg, 1976; Kingsley and Watabe, 1982b; 1984; this paper), gastropod sherules (Abolins-Krogis, 1970; Watabe et al., 1976) and polychaete opercula and tubes (Neff, 1971; Bubel, 1983). The extracellular stage of spine and test formation involves secondary sclerocytes that do not form calcifying vacuoles, but as in our study, form elongated cytoplasmic extensions or thin membranes over the crystal surface.

A proposal for the multicellular origin of gorgonian spicules has been made previously by most all earlier workers using light microscopy. As stated by Chester (1913), "the formation of the spicules is not different from that described by von Koch (1897), Bourne (1899) or Woodland (1905). The more or less rounded spicule-cell first shows a small calcareous mass which increases in size with the division of the cell and takes on a characteristic shape. Several nuclei are to be found in the cytoplasm enveloping most of the spicules, thus showing that the spicule-cell usually divides more than once." A multicellular origin is also implied by tissue culture studies of spicule formation (Rannou, 1968) and by some electron microscopic evidence (Kawaguti, 1964; Kawaguti and Kamishima, 1973). However, more detailed electron microscopic work suggests that spicule formation occurs in single cells (Kawaguti, 1969; Dunkelburger and Watabe, 1974; Kingsley and Watabe, 1982b; Kingsley, 1984). It is clearly possible that some species differ in this regard. However, when only electron microscopy is used to examine large scale phenomena, additional problems are introduced. Cells with meandering plasma membranes, and nuclei separated by large volumes of mineralized material are difficult to prepare and may be difficult to interpret. Spicules of different shapes

and varying degrees of complexity are found within the same colony. In many cases, spicular morphology is a function of the region in the colony where the spicule was formed (Bayer, 1961). We have not examined the origin of all spicular types in *Pseudoplexaura flagellosa* and cannot state with certainty that all spicules in this species have a complex origin; it is possible, for example, that the relatively simple spicules found in the polyps differ in this regard from those formed in the coenenchyme.

Since the spiculation of gorgonians and other Octocorallia is species-specific and forms the basis of their taxonomy (Bayer, 1961), genetic controls must govern the features of spicule formation. Although a discussion of such controls is beyond the scope of this paper, two features of spicule formation deserve special mention. We have noted that primary sclerocytes proliferate during early stages of regeneration and are otherwise uncommon. We have also noted that these cells produce primordia of different size and possibly of different configuration due to variation in crystal shape. Thus, primary sclerocytes may not only limit the number of spicules produced but may influence the form of their secondary growth as well. A profusion of primary sclerocytes might also occur under certain pathogenic conditions known to produce abnormally large numbers of spicules (Goldberg et al., 1984).

Mesoglea may also play a critical role in spicule organization, especially in stages where secondary sclerocytes are not in direct contact (Figs. 11–13). In these later stages, spicules and component cells are connected by mesogleal fibers and are separated from other nascent spicules by compartments within the mesogleal matrix (Fig. 14). As a connective tissue, mesoglea has a number of roles suited to extracellular organization. It is both an adhesive to which cells may adhere chemically and physically, and is a substrate over which migration may be directed (Hausman, 1973). Its similarity to basement membrane has been documented (Barzansky et al., 1975) and its role in regeneration, cellular migration and morphogenesis has been the subject of a number of investigations (Chapman, 1974; Campbell, 1974; Day and Lenhoff, 1981; Novak and Wood, 1983). Some experimental evidence suggests organization of cells by extracellular matrix protein during spicule formation in echinoderms (Benson and Blankenship, 1982). Tissue culture studies will be necessary to delineate a similar role for mesoglea.

The necessity of employing decalcification procedures in electron microscopy causes several related problems. First, the decalcifying agent often distorts tissue, causing loss of membrane definition, shrinkage, cell separation and extraction of cytoplasmic components. Part of this may be due to the effect of the demineralizing solute (e.g., acid or chelating agent), and part to the solvent effects that accompany prolonged decalcification procedures (Dietrich and Fontaine, 1975). A number of authors have examined variations in solute and solvent in an attempt to deal with this problem. The most commonly used decalcifying solute, EDTA, has the advantage of being prepared in ethanol. Ethanolic decalcification appears in many cases to deal adequately with solvent effects (Scott and Kyffin, 1978; Dickson and Jande, 1980; Scott and Burton, 1984; this study) even though more time for decalcification is required compared with aqueous EDTA.

The other major problem related to decalcification procedures is adequate fixation of tissue. The fixatives most commonly employed in electron microscopy are various aldehydes and osmium tetroxide, neither of which reacts directly with most polysaccharides (Hayat, 1975; 1981; Bullock, 1983). Glycoproteins, proteoglycans and acidic polysaccharides are often associated with calcified matrices and are especially susceptible to extraction. A number of studies have shown that

several substances can be added to standard fixative mixtures to enhance retention of these matrix components. Such additives include diamines (Boyles, 1984), quaternary ammonium compounds (Shea, 1971; Crenshaw and Ristedt, 1976), tannic acid (Sannes et al., 1978; Singley and Solursh, 1980) and various cationic dyes. The most commonly employed among the latter group include alcian blue Behnke and Zelander, 1970; Ruggeri et al., 1975) and ruthenium red (Luft, 1971a, 1971b), although other dyes including toluidine blue, acridine orange and cuprolinic blue have also been used (Van Kuppevelt et al., 1984 and contained references). All of these substances bind polyanionic material and when used in conjunction with glutaraldehyde, preserve the ultrastructure of matrix glycans. In many cases, the glycan–dye–aldehyde complex is also osmiophilic (Behnke and Zelander, 1970; Luft, 1971b; Hayat, 1975), further enhancing contrast. In the case of alcian blue and ruthenium red, this fixation and contrast enhancement of carbohydrate is usually restricted to the extracellular space. However, this is not always the case and much appears to depend upon the type of cell, conditions of fixation and other variables employed in specimen preparation (Hayat, 1975). Nonetheless, this general inability of RR to penetrate cell membranes has been used by Shimizu and Yamada (1980) to demonstrate intracellular versus extracellular processes associated with calcification. Similarly, our data suggest that RR preserves the matrix of decalcified spicules extracellularly, but is generally excluded from interaction with intracellular matrices. This exclusion may be a function of the calcifying vesicle membrane, rather than the plasma membrane of the sclerocyte. RR-fixed sclerocytes show enhanced contrast of all membranes within the cell, and display an increased electron density in the Golgi apparatus and the mitochondria (Fig. 4).

The chemistry of the spicular matrix has yet to be examined in this species but preliminary work with isolated spicules suggests that decalcification ordinarily destabilizes the matrix. Preservation of the insoluble (visible) fraction is related primarily to fixation with ruthenium red and secondarily to the nature of the decalcifying agent. The presence of aldehyde during decalcification has no effect on retaining greater amounts of spicular matrix, nor does fixation with osmium since the matrix is not osmiophilic. There appears to be at least some solubilization of matrix during decalcification irrespective of procedure. Such problems of fixation may be relevant to our inability to describe the morphological details of crystal formation; they may also account for the predominant absence of an intracrystalline matrix in decalcified preparations. While this degree of lability appears to be exceptional, the use of ruthenium red prior to decalcification has enabled us to preserve the crystal outlines as well as the overall form of the spicule for microscopic examination.

Acknowledgments

This work was supported by a Weitzmann Postdoctoral Fellowship (to Y.B.). We thank M. Goreau, University of Miami, for elemental analysis of whole spicules and N. Watabe, University of South Carolina, for critical reviews that considerably improved the quality of this work during its developmental stages. We thank C. Bigger, FIU, for critical review of the manuscript, and R. Graham for drafting the illustrations.

Literature Cited

Abolins-Krogis, A. 1970. Electron microscope studies of the intracellular origin and formation of calcifying granules and calcium spherites in the hepatopancreas of the snail, *Helix pommatia* (L.). Z. Zellforsch. Microsk. Anat. 108: 501–515.

Alsop, D. W. 1974. Rapid single-solution polychrome staining of semithin epoxy sections using polyethylene glycol 200 (PEG 200) as a stain solvent. Stain Technol. 49: 265–272.

Barzansky, B., H. M. Lenhoff and H. Bode. 1975. Hydra mesoglea: similarity of its amino acid and neutral sugar composition to that of vertebrate basal lamina. Comp. Biochem. Physiol. 50B: 419–424.

Bayer, F. M. 1955. Contributions to the nomenclature, systematics and morphology of the Octocorallia. Proc. U.S. Natl. Mus. 105: 207–220.

———. 1961. The shallow-water Octocorallia of the West Indian region. Martinus Nijhoff, The Hague, Netherlands. 373 pp.

Behnke, O. and T. Zelander. 1970. Preservation of intercellular substances by the cationic dye alcian blue in preparative procedures for electron microscopy. J. Ultrastr. Res. 34: 424–438.

Benson, S. C. and J. Blankenship. 1982. Relationship between collagen metabolism and spicule formation in sea urchin micromeres. J. Cell Biol. 95: 158 (abstr.).

Bonucci, E. and J. Reurink. 1978. The fine structure of decalcified cartilage and bone: a comparison between decalcification procedures performed before and after embedding. Calcif. Tiss. Res. 25: 179–190.

Boyles, J. 1984. The use of primary amines to improve glutaraldehyde fixation. Pages 7–21 *in* J. P. Revel, T. Barnard and G. H. Haggis, eds. Science of biological specimen preparation. SEM, Inc., AMF O'Hare, Chicago.

Bubel, A. 1983. A fine structural study of the calcareous opercular plate and associated cells of a polychaete annelid. Tiss. Cell 15: 457–476.

Bullock, G. R. 1983. The current status of fixation for electron microscopy: a review. J. Microsc. 133: 1–15.

Campbell, R. D. 1974. Development. Pages 179–210 *in* L. Muscatine and H. M. Lenhoff, eds. Coelenterate biology reviews and new perspectives. Academic Press, New York.

Chapman, G. 1974. The skeletal system. Pages 93–128 *in* L. Muscatine and H. M. Lenhoff, eds. Coelenterate biology reviews and new perspectives. Academic Press, New York.

Chester, W. M. 1913. The structure of *Pseudoplexaura crassa* Wright and Studer. Proc. Amer. Acad. Arts Sci. 48: 737–781.

Crenshaw, M. A. and H. Ristedt. 1976. The histochemical localization of reactive groups in septal nacre from *Nautilus pompilius* L. Pages 355–367 *in* N. Watabe and K. M. Wilbur, eds. The mechanisms of mineralization in the invertebrates and plants. University of South Carolina Press, Columbia, S.C.

Day, R. M. and H. M. Lenhoff. 1981. Hydra mesoglea: epithelial cell-basement membrane interactions. Science 211: 291–294.

Dickson, I. R. and S. S. Jande. 1980. Effects of demineralization in an ethanolic solution of triethylammonium EDTA on solubility of bone matrix components and on ultrastructural preservation. Calcif. Tiss. Int. 32: 175–179.

Dietrich, H. F. and A. R. Fontaine. 1975. A decalcification method for ultrastructure of echinoderm tissues. Stain Technol. 50: 351–354.

Dunkelberger, D. G. and N. Watabe. 1974. An ultrastructural study on spicule formation in the pennatulid colony *Renilla reniformis*. Tiss. Cell 6: 573–586.

Franc, S., A. Huc and G. Chassagne. 1974. Étude ultrastructurale et physico-chemique de l'axe squelettique de *Veretillum cynomorium* Pall. (Cnidaire, Anthozoaire): cellules, calcite collagène. J. Microscopie 21: 93–100.

Grasshoff, M. and H. Zibrowius. 1983. Kalkkrusten auf Achsen von Hornkorallen, rezent und fossil (Cnidaria, Anthozoa, Gorgonaria). Senckenberg. Marit. 16: 111–145.

Goldberg, W. M., J. C. Makemson and S. B. Colley. 1984. *Entocladia endozoica* sp. nov., a pathogenic chlorophyte: structure, life history, physiology, and effect on its coral host. Biol. Bull. 166: 368–383.

Hausman, R. E. 1973. The mesoglea. Pages 393–453 *in* A. L. Burnett, ed. Biology of Hydra. Academic Press, New York.

Hayat, M. A. 1975. Positive staining for electron microscopy. Van Nostrand Reinhold Company, New York. Pp. 162–176.

———. 1981. Fixation for electron microscopy. Academic Press, New York. Pp. 64–147.

Ito, S. and M. J. Karnovsky. 1968. Formaldehyde-glutaraldehyde fixatives containing trinitro compounds. J. Cell Biol. 39: 168a–169a.

Kawaguti, S. 1964. Electron microscopy on the spicules and the polyp of the gorgonian *Euplexaura erecta*. Biol. J. Okayama Univ. 10: 23–28.

———. 1969. Electron microscopy on a soft coral, *Heteroxenia elisabethae* Kölliker. Biol. J. Okayama Univ. 15: 25–35.

——— and Y. Kamishima. 1973. Electron microscopy on a gorgonian coral, *Anthoplexaura dimorpha*. Publ. Seto Mar. Biol. Lab. 20: 785–793.

Kingsley, R. J. 1984. Spicule formation in the invertebrates with special reference to the gorgonian *Leptogorgia virgulata*. Am. Zool. 24: 883–891.

——— and N. Watabe. 1982a. Ultrastructure of the axial region in *Leptogorgia virgulata* (Cnidaria: Gorgonacea). Trans. Am. Microsc. Soc. 101: 325–339.

——— and ———. 1982b. Ultrastructural investigation of spicule formation in the gorgonian *Leptogorgia virgulata* (Lamarck) (Coelenterata, Gorgonacea). Cell Tiss. Res. 223: 325–334.

——— and ———. 1984. Synthesis and transport of the organic matrix of the spicules in the gorgonian *Leptogorgia virgulata* (Lamarck) (Coelenterata: Gorgonacea). An autoradiographic investigation. Cell Tiss. Res. 235: 533–538.

Ledger, P. W. and S. Franc. 1978. Calcification of the collagenous axial skeleton of *Veretillum cynomorium* Pall. (Cnidaria: Pennatulacea). Cell Tiss. Res. 192: 249–266.

Luft, J. H. 1971a. Ruthenium red and violet: I. Chemistry, purification, methods of use for electron microscopy and mechanism of action. Anat. Rec. 171: 347–368.

———. 1971b. Ruthenium red and violet: II. Fine structural localization in animal tissues. Anat. Rec. 171: 369–416.

Märkel, K. and U. Röser. 1983. The spine tissues in the echinoid *Eucidaris tribuloides*. Zoomorph. 103: 25–41.

Neff, J. M. 1971. Ultrastructural studies of the secretion of calcium carbonate by the serpulid polychaete worm, *Pomatoceros caerulens*. Z. Zellforsch. Mikrosk. Anat. 120: 160–186.

Novak, P. L. and R. L. Wood. 1983. Development of the nematocyte junctional complex in *Hydra* tentacles in relation to cellular recognition and positioning. J. Ultrastr. Res. 83: 111–121.

Rannou, M. 1968. Formation de spicules dans des cultures cellulaires de cnidare (gorgone). Vie et Milieu 19: 53–58.

Ruggeri, A., C. Dell'orbo and D. Quacci. 1975. Electron microscopic visualization of proteoglycans with alcian blue. Histochem. J. 7: 187–197.

Sannes, P. L., T. Katsuyama and S. S. Spicer. 1978. Tannic acid-metal salt sequences for light and electron microscopic localization of complex carbohydrates. J. Histochem. Cytochem. 26: 55–61.

Scott, J. E. and S. M. Burton. 1984. Selective demineralization of hard tissues in organic solvents: retention or extraction of proteoglycan? J. Microsc. 134: 291–297.

——— and T. W. Kyffin. 1978. Demineralization in organic solvents by alkylammonium salts of ethylenediaminetetraacetic acid. Biochem. J. 169: 697–701.

Shea, S. M. 1971. Lanthanum staining of the surface coat of cells. Its enhancement by the use of fixatives containing alcian blue or cetylpyridinium chloride. J. Cell Biol. 51: 611–620.

Shepard, N. and N. Mitchell. 1977. The use of ruthenium red and p-phenylenediamine to stain cartilage simultaneously for light and electron microscopy. J. Histochem. Cytochem. 25: 1163–1168.

Shimizu, M. and J. Yamada. 1980. Sclerocytes and crystal growth in the regeneration of sea urchin test and spines. Pages 169–178 *in* M. Omori and N. Watabe, eds. The mechanisms of biomineralization in animals and plants. Tokai University Press, Tokyo.

Simionescu, N. and M. Simionescu. 1976. Galloylglucoses of low molecular weight as mordant in electron microscopy. J. Cell Biol. 70: 608–621.

Singley, C. T. and M. Solursh. 1980. The use of tannic acid for the ultrastructural visualization of hyaluronic acid. Histochemistry 65: 93–102.

Spangenberg, D. 1976. Intracellular statolith synthesis in *Aurelia aurita*. Pages 231–248 *in* N. Watabe and K. M. Wilbur, eds. The mechanisms of mineralization in the invertebrates and plants. University of South Carolina Press, Columbia.

Stricker, S. A. 1985. The ultrastructure and formation of the calcareous ossicles in the body wall of the sea cucumber *Leptosynapta clarki* (Echinodermata, Holothuroidea). Zoomorphology 105: 209–222.

Van Kuppevelt, T., J. Domen, F. Cremers and C. Kuyper. 1984. Staining of proteoglycans in mouse lung alveoli I. Ultrastructural localization of anionic sites. Histochem. J. 16: 657–669.

Wakita, M., M. Kobayashi and T. Shioi. 1983. Decalcification for electron microscopy with L-ascorbic acid. Stain Technol. 58: 337–341.

Watabe, N., V. R. Meenakshi, P. L. Blackwelder, E. M. Kurtz and D. G. Dunkelberger. 1976. Calcareous splerules in the gastropod *Pomacea paludosa*. Pages 238–308 *in* N. Watabe and K. M. Wilbur, eds. The mechanisms of mineralization in the invertebrates and plants. University of South Carolina Press, Columbia.

Wilbur, K. M. 1980. Cells, crystals and skeletons. Pages 1–11 *in* M. Omori and N. Watabe, eds. The mechanisms of biomineralization in animals and plants. Tokai University Press, Tokyo.

——— and K. Simkiss. 1979. Carbonate turnover and deposition by Metazoa. Pages 69–106 *in* P.

A. Trudinger and D. J. Swaine, eds. Biogeochemical cycling of mineral-forming elements. Elsevier Sci. Pub. Co., New York.

DATE ACCEPTED: March 4, 1986.

ADDRESSES: *(W.M.G.) Dept. of Biological Sciences, Florida International University, Tamiami Campus, Miami, Florida 33199; (Y.B.) Dept. of Zoology, Tel-Aviv University, Ramat-Aviv, Tel-Aviv, Israel.*